

1 **Robust future precipitation declines in CMIP5 largely reflect the poleward expansion of model**  
2 **subtropical dry zones**

3

4

5 Jack Scheff and Dargan M. W. Frierson, Department of Atmospheric Sciences, University of  
6 Washington, Box 351640, Seattle, WA 98195-1640, USA. (jscheff@uw.edu)

7

## 8 Key points

9 -New climate models expand their subtropical dry zones poleward with warming

10 -Poleward retreat of midlatitude precipitation explains most multimodel drying

11 -The extent of robust drying has strong spring-fall and wavenumber-1 asymmetries

## 12 Abstract

13 Robust subtropical precipitation declines have been a prominent feature of general circulation  
14 model (GCM) responses to future greenhouse warming. Recent work by the authors showed that for  
15 the models making up the Coupled Model Intercomparison Project phase 3 (CMIP3), this drying was  
16 found mainly in the midlatitude-driven precipitation poleward of the model subtropical precipitation  
17 minima. Here, using more comprehensive diagnostics, we extend that work to 32 new CMIP5 models,  
18 and find that CMIP5 robust precipitation declines are also found mainly between subtropical minima  
19 and midlatitude precipitation maxima, implicating dynamic poleward expansion of dry zones rather  
20 than thermodynamic amplification of dry-wet contrasts. We also give the full seasonal cycle of these  
21 projected declines, showing that they are much more widespread in local spring than in local fall, and  
22 that for most of the year in the Northern Hemisphere they are entirely confined to the Atlantic side of  
23 the globe.

24 **Index terms:** Atmospheric Processes: Water Cycles; Atmospheric Processes: Climate Change &  
25 Variability; Atmospheric Processes: Climate Dynamics; Atmospheric Processes: Global Climate  
26 Models; Computational Geophysics: Data Presentation and Visualization

27 **Keywords:** subtropical drying, subtropical dry zones, mid-latitude precipitation, poleward expansion,  
28 poleward shift, dry-get-drier

## 29 1. Introduction

30 Since at least the middle of the last decade, it has been noted that most general circulation  
31 models (GCMs) agree on certain aspects of the large-scale precipitation (P) response to strong  
32 greenhouse-driven global warming [e.g. *Meehl et al.*, 2007b; *Held and Soden*, 2006; *McSweeney and*

33 *Jones, 2012*]. These robust responses include increases in much of the high latitudes and parts of the  
34 deep tropics; and decreases in large areas of the subtropics, which have elicited particular concern [e.g.  
35 *Seager et al., 2007; Hansen et al., 2008*].

36 Two distinct causes have been identified for the subtropical P decreases, at least in the models  
37 of the Coupled Model Intercomparison Project (CMIP) phase 3 (CMIP3) multimodel archive [*Meehl et*  
38 *al., 2007a*]. *Held and Soden* [2006], as well as *Seager et al.* [2010] showed amplification of the  
39 multimodel-mean field of precipitation minus actual evaporation (P-E), with positive P-E regions  
40 becoming more positive, and negative P-E regions (i.e. subtropical oceans) becoming more negative, as  
41 a simple consequence of the Clausius-Clapeyron increase in vapor transport in a warmer future world  
42 [e.g. *Manabe and Wetherald, 1975*]. *Held and Soden* [2006] argued that these P-E changes are largely  
43 accomplished by P changes. Thus, all else equal, they suggest that models will tend to reduce P  
44 wherever  $P < E$ , including the subtropical dry margins of both the tropical wet belt and of the  
45 midlatitude storm tracks.

46 Meanwhile, a number of studies [e.g. *Yin, 2005; Lorenz and DeWeaver, 2007; Lu et al., 2007;*  
47 *Previdi and Liepert, 2007*] noted that in almost every CMIP3 model, the midlatitude storm tracks and  
48 jets shift poleward with 21st-century greenhouse warming, and the subtropical dry zones and  
49 descending Hadley-Ferrel branches expand poleward in their wake. In contrast to the above  
50 mechanism, this less well understood dynamical response should mainly act to reduce P poleward of  
51 the subtropical P minima (potentially including wet regions as well as dry), and not on the dry margins  
52 of the tropical wet belt.

53 In *Scheff and Frierson* [2012; hereafter SF12], the present authors showed that the robust future  
54 P reductions in the CMIP3 model subtropics are almost entirely located in midlatitude-driven P  
55 poleward of the model P minima, suggesting that their main cause is this poleward expansion of the dry  
56 zones, and not the thermodynamic “dry-get-drier” mechanism described above. In the present study,  
57 we extend the SF12 methods and results to 32 new models in the CMIP phase 5 multimodel archive

58 [*Taylor et al.*, 2012] (listed in table 1), further clarify the seasonal, hemispheric and regional variation  
59 in the results, and note some of the few differences between CMIP5 and CMIP3.

## 60 **2. Results**

### 61 2.1. All models on the same grid

62 Figure 1 depicts, for each point on a common  $\frac{1}{4} \times \frac{1}{4}$  degree grid, the multimodel statistics of the  
63 21st-century (1980-2099) trends of seasonal P in the native model gridboxes containing that point. All  
64 trends and significances are defined as in SF12, but using the CMIP5 scenarios “historical” and  
65 “rcp8.5”. As shown in the legend, bold blue colors mean that almost all 32 CMIP5 models in table 1  
66 significantly increase P, bold red colors mean that almost all models significantly decrease P, and very  
67 light or white colors mean that few or no models have a significant trend in P. In contrast, pastel  
68 (and/or purple) hues represent disagreement within CMIP5 on the presence (and/or sign) of a  
69 significant model-gridbox-scale P response. The multimodel-mean late 20th-century (1980-1999) P  
70 climatology (computed as in SF12) is plotted as a reference, with thicker black contours corresponding  
71 to higher values of seasonal climatological P.

72 The CMIP5 seasonal P responses feature robust increases throughout almost all of the higher  
73 latitudes and in certain parts of the wet tropics, with robust declines in large portions of the subtropics,  
74 as in the CMIP3 work cited in section 1. Furthermore, the declines (bold red) are largely found in  
75 regions of baroclinically forced P, between the multimodel subtropical P minima and midlatitude P  
76 maxima. This is just what SF12 found for CMIP3, reinforcing the conclusion that these P decreases  
77 mainly reflect the poleward expansion of the seasonal model dry zones toward the midlatitudes. If  
78 anything, the declines tend to be even more robust in CMIP5 than in CMIP3, especially in the Southern  
79 Hemisphere in winter and spring (figures 1c-d). The equivalent plots for the 19 CMIP3 models  
80 examined in SF12 are presented as Supplementary Figure S1.

81 In contrast, the central portions of the subtropical dry zones tend to be mottled with various  
82 lighter shades in figure 1, implying a lack of robustness in P response. Meanwhile, the tropical dry

83 margins further equatorward show all sorts of responses, from robust drying (e.g. north of the east  
84 Pacific ITCZ in spring, figure 1b) to robust wetting (e.g. in the Horn of Africa north of the ITCZ in  
85 boreal winter, figure 1a) to robust insignificance (e.g. south of the Indian Ocean ITCZ in winter, figure  
86 1c), and everything in between. Thus, the simple “dry-get-drier” rule from the amplified vapor  
87 transport does not appear to be in phase with the CMIP5 P responses. Instead, the dynamical replacement  
88 of midlatitude wetness with subtropical dryness and descent offers a much cleaner explanation for the  
89 robust subtropical P declines, as in SF12.

90       Furthermore, and also as in SF12, the high-latitude robust wetting in figure 1 is often located  
91 directly across the climatological midlatitude wet belt from the subtropical robust drying (e.g.  
92 throughout the Southern Hemisphere in all seasons, or in the north Pacific in winter), so that the robust  
93 P response pattern is in near-quadrature with the multimodel climatology in the extratropics. This  
94 phase relationship suggests a poleward shift of certain midlatitude storm tracks as a key element of P  
95 changes in CMIP5.

96       This general pattern does have some local exceptions, many of which are more robust in CMIP5  
97 (figure 1) than in CMIP3 (figure S1). Notably, the region north of the ITCZ in the American sector  
98 often features robust P decreases that fully straddle the subtropical dry belt (e.g. the western subtropical  
99 north Atlantic in winter, or the Caribbean in summer.) The Southern Hemisphere in springtime (figure  
100 1d) sees some similar “dry-get-drier” robust decreases as well, most notably in southern Africa.  
101 However, the overall impression remains that subtropical P declines in CMIP5, as in CMIP3, are  
102 dominant *poleward* of the driest zones, i.e. in extratropical-forced P. In fact, many of the above  
103 exceptions are situated at regional saddles in the P field, where midlatitude and tropical P zones appear  
104 to connect or overlap, so that they might also be conceivably driven by the poleward retreat of  
105 extratropical dynamic P forcing. *Tyson and Preston-Whyte* [2000] details the frontal production of  
106 springtime southern-African P in particular.

107       Interestingly, there is also a pronounced spring-fall asymmetry (compare figures 1b and 1d) in

108 both hemispheres, with drying more prevalent in local spring. This was already noted for the monsoon  
109 regions by *Seth et al.* [2011] for CMIP3 and by *Seth et al.* [2012] for CMIP5; however figure 1 makes  
110 it clear that this is a broader phenomenon extending across much of the subtropics and midlatitudes.  
111 The reason for this consistent asymmetry is unclear, since the *Seth et al.* explanation of reduced low-  
112 level moisture supply at the end of a warmer future dry season is only applicable over land. However,  
113 it is still a noticeable pattern that demands explanation.

## 114 2.2. Model-by-model approach

115 The above interpretation using the multimodel climatology as a reference may be misleading  
116 for individual, biased models, because their own climatological dry and wet zones may be located in  
117 different latitudes than those of the ensemble mean. In SF12, we introduced a novel system for  
118 recording each CMIP3 model's seasonal P response pattern relative to the pattern of its *own*  
119 climatology in a uniform fashion that can be collated across many models.

120 In Figure 2, we apply this method to the CMIP5 models to confirm the results in section 2.1. In  
121 each seasonal panel of figure 2, the horizontal axis marks off thirty-six 10°-longitude-wide bands,  
122 zonally spanning the globe. Each band supports a vertical column of boxes colored as in figure 1,  
123 stretching from “South Pole Min” up to “North Pole Min”, and interrupted at the ITCZ(s) for visual  
124 clarity. As in figure 1, the colors indicate how many models have significantly increasing, significantly  
125 decreasing, or insignificant 21st-century P trends.

126 The key aspect of this method is that in each of these columns, the correspondence between the  
127 vertical “coordinate” and actual local latitude is determined *separately* for *each model*, using that  
128 model’s own late-20th-century P climatology. Thus, for example, the bluish color in figure 2a in the  
129 leftmost longitude band at the north midlatitude maximum means that many individual CMIP5 models  
130 respond to rcp8.5 with significant December-February 0-10°E P increases at the latitude of *their*  
131 present-day December-February 0-10°E north midlatitude P maximum, *whatever that latitude is for*  
132 *each model*. For more details, see the appendix, and/or SF12.

133 As in SF12, the pattern is broadly similar to that found with the fixed-grid approach, but clearer,  
134 and more credible due to this spatial bias removal. In particular, the Southern Hemisphere of figure 2  
135 in each season strongly supports the conclusions from section 2.1, with the robust P reductions  
136 characterizing not the models' subtropical P minima and vicinity, but rather the broad belts between  
137 those minima and the midlatitude P maxima (including both dry and wet regions.) This is most  
138 remarkably so in summer and fall (figures 2a-b) but still holds well in the other seasons, though the  
139 exception noted in section 2.1 near southern Africa ( $10^{\circ}$ - $50^{\circ}$  longitude or so) in spring (figure 2d) is  
140 still apparent.

141 The meridional quadrature pattern noted in section 2.1, with bold blues located directly across  
142 the models' southern midlatitude P maxima from the bold reds, is perhaps even more striking in this  
143 view than in figure 1, and again strongly suggests a poleward shift of southern midlatitude precipitation  
144 in all seasons in response to future global warming in CMIP5. In contrast, the signals at and  
145 equatorward of the south subtropical minima are varied and usually non-robust, even in wet tropical  
146 zones near the (south) ITCZ. In short, the Southern Hemisphere robust P response in this framework  
147 looks much more like dynamic poleward expansion of dryness into the midlatitudes than  
148 thermodynamic "dry-get-drier," just as in section 2.1 and in SF12.

149 In the Northern Hemisphere, though, figure 2 is more ambiguous. In each season, the Europe-  
150 Africa region (roughly  $340^{\circ}$ - $050^{\circ}$  longitude) responds just like the Southern Hemisphere above – the  
151 subtropical dry zones expand poleward without any robust drying in the tropical dry margins (or wet  
152 tropics). This also characterizes the northwest Pacific ( $130^{\circ}$ - $190^{\circ}$ ) in winter only (figure 2a), and the  
153 north subtropical Atlantic ( $270^{\circ}$ - $340^{\circ}$ ) in spring only (figure 2b). However, the American/Atlantic  
154 sector (roughly  $210^{\circ}$ - $330^{\circ}$ ) always contains a similarly broad drying region centered on or equatorward  
155 of the P minimum. Meanwhile, through most of the year (figures 2b-d) the Asian continent and  
156 neighboring Pacific ( $50^{\circ}$ - $190^{\circ}$ ) don't show any robust P declines at all, in *any* feature-relative  
157 "location" (nor in any real location on figures 1b-d for that matter), subtropical or otherwise.

158 So, in the Northern Hemisphere, which (if any) type of subtropical drying appears to dominate  
159 the CMIP5 responses is a strong and somewhat seasonally invariant function of longitude. This quasi-  
160 wavenumber-1 asymmetry was discussed briefly in section 2.1 above and in SF12, but this view makes  
161 it clearer. Poleward expansion is still the most common Northern Hemisphere drying type overall, but  
162 not near-universally as in the Southern Hemisphere.

163 Figure 2 also reproduces the curious spring-fall asymmetry seen in figure 1, especially in the  
164 Northern Hemisphere, where the extent of robust drying in local fall (figure 2d) is strikingly low  
165 compared to the other seasons.

166 Finally, the equivalent of figure 2 for the SF12 CMIP3 models is provided as Supplementary  
167 Figure S2 for comparison. The greater robustness of Southern Hemisphere winter-spring drying in  
168 CMIP5 than in CMIP3, noted for figures 1 and S1, is reaffirmed. Similarly, the local robust “dry-get-  
169 drier” responses found in southern Africa (and parts of South America) in local spring and in the  
170 subtropical North Atlantic in local winter are largely *novel* features of CMIP5, as suggested in section  
171 2.1. (Other CMIP5 “dry-get-drier” regions were robust in CMIP3, especially near the Americas north  
172 of the ITCZ(s) [SF12]).

### 173 **3. Summary and discussion**

174 In a previous study, the authors [SF12] used one established and one novel diagnostic method to  
175 argue that robust local precipitation (P) decline due to future global warming in 19 CMIP3 GCMs was  
176 largely an extratropical phenomenon, associated with the poleward expansion of the individual GCMs'  
177 subtropical low-P zones. In section 2 above, the SF12 techniques were improved and extended to 32  
178 new CMIP5 models, and the CMIP3 result was strongly reaffirmed. Aspects of the result's seasonal  
179 cycle involving local spring and fall (in addition to summer and winter) were clarified, and regional  
180 exceptions to the overall result were noted.

181 It is instructive to consider why P declines roughly centered on the subtropical dry minima  
182 themselves (“dry-get-drier” decreases), expected from basic moist theory, are not more widespread.



183 *Held and Soden* [2006], *Seager et al.* [2010], SF12, and others show that P-E does decrease in these  
184 regions in most CMIP3 models, and SF12 shows that this doesn't translate to robust P declines,  
185 implying a role for E increases in balancing the increased vapor flux divergence. Both of these  
186 properties can be confirmed in CMIP5 to some degree using the SF12 diagnostics (not shown.)  
187 However, *Seager et al.* [2010] show that P-E itself does not decrease so strongly on the tropical dry  
188 margins, due to the slowdown of the tropical circulation to conserve energy under global warming [e.g.  
189 *Vecchi and Soden, 2007; Held and Soden, 2006*]. Furthermore, *Neelin et al.* [2006] note the  
190 inconsistency of P response to global warming on the tropical dry margins, as different regions and  
191 models see the wet ITCZ either advance toward the subtropical dry region, or retreat away from it.  
192 Thus, it is plausible that the dry-get-drier mechanism is still working to reduce P, but that the above  
193 factors combine to cancel and/or overwhelm this signal in the lower-latitude portions of the dry  
194 subtropics, leaving the midlatitude flanks as the robust loci of thermodynamic P reduction. However,  
195 this still does not explain why the reductions often extend poleward all the way to the midlatitude wet  
196 maxima, with P increases situated poleward of the maxima (the shift-dominated pattern discussed in  
197 section 2). In any case, it seems simpler to describe the robust model P decreases as poleward retreat  
198 of some extratropically-driven P (affecting both present-day dry and wet regions) than as amplification  
199 of dry-wet contrasts.

## 200 **Appendix**

201       The precise meaning of the vertical axes in figures 2 and S2 is as follows: for each model, in  
202 each season and each of the thirty-six 10°-longitude-wide bands, we use criteria defined in SF12 (with  
203 one minor difference, explained below) to identify the latitudes of the tropical ITCZ peak(s) and (if  
204 possible) the subtropical minima and midlatitude peaks of the 10°-zonal-mean late 20th century P. If  
205 these latter two features are present in either hemisphere, then every latitude between the pole and the  
206 (nearest) ITCZ is classified according to which two features it lies between, and then according to its  
207 10°-zonal-mean late 20th century model P value relative to those two features. For example, all model

208 latitudes lying between the model's 0-10°E December-February subtropical minimum and midlatitude  
209 maximum, and whose 0-10°E December-February P is between 2/6 and 3/6 of the way from the former  
210 to the latter, are binned together. In each such bin, we then note the fraction of latitudes for which the  
211 21st-century trend in the model's 10°-zonal-mean P is significant and upward, and similar for  
212 insignificant and for significant and downward. For each model, these fractions are usually either zero  
213 or unity, since the bins usually contain latitudes that are close together and behave similarly.

214 This entire procedure is then repeated separately for each model, and the above fractions are  
215 averaged across all applicable models at the same relative bin-definition (i.e. same vertical coordinate  
216 in figures 2 and S2) to obtain the fractions color-plotted in figures 2 and S2. Because the individual-  
217 model fractions are usually zero or unity, the averages can be thought of as the proportion of *models*  
218 that dry, wet, or leave P unchanged under rcp8.5 global warming in whichever individual-model  
219 latitudes are locally represented. For a more detailed version of these two paragraphs, see SF12.

220 The small difference between the P feature definition criteria used here and those used in SF12,  
221 mentioned above, is as follows: for a given hemisphere (north or south), we now declare these features  
222 locally absent if the putative subtropical minimum falls poleward of 55° latitude, not 66.5°. This  
223 stricter criterion eliminates clear false positives in the warm season in the vicinity of far-eastern Siberia  
224 and the Sea of Okhotsk, and does not introduce any false negatives. (For features of the *P-E* field, we  
225 still recommend the original value of 66.5°.)

## 226 **Acknowledgements**

227 The authors acknowledge the World Climate Research Programme's Working Group on  
228 Coupled Modelling, which is responsible for CMIP, and we thank the climate modeling groups listed in  
229 table 1 for producing and making available their model output. For CMIP, the U.S. Department of  
230 Energy's Program for Climate Model Diagnosis and Intercomparison provides coordinating support  
231 and leads development of software infrastructure in partnership with the Global Organization for Earth  
232 System Science Portals. Also, the authors would like to thank M. Pritchard for graphical inspiration.

233 This work is funded by NSF grants ATM-0846641 and ATM-0936059.

234 **References**

235 Hansen, J., and co-authors (2008), Target atmospheric CO<sub>2</sub>: where should humanity aim?, *Open Atmos.*  
236 *Sci. J.*, 2, 217-231.

237 Held, I., and B. Soden (2006), Robust responses of the hydrological cycle to global warming, *J. Clim.*,  
238 *19*, 5686-5699.

239 Lorenz, D. J., and E. T. DeWeaver (2007), Tropopause height and zonal wind response to global  
240 warming in the IPCC scenario integrations, *J. Geophys. Res.*, *112*, D10119,  
241 doi:10.1029/2006JD008087.

242 Lu, J., G. A. Vecchi, and T. J. Reichler (2007), Expansion of the Hadley cell under global warming,  
243 *Geophys. Res. Lett.*, *34*, L06805, doi:10.1029/2006GL028443.

244 Manabe, S., and R. T. Wetherald (1975), The effects of doubling the CO<sub>2</sub> concentration on the climate  
245 of a general circulation model, *J. Atmos. Sci.*, *32*, 3-15.

246 McSweeney, C., and R. Jones (2012), Consensus and confidence: measuring, communicating and  
247 interpreting model ensemble agreement, paper presented at WCRP Workshop on CMIP5 Model  
248 Analysis, World Clim. Res. Prog., Honolulu, Hawaii.

249 Meehl, G. A., C. Covey, T. Delworth, M. Latif, B. McAvaney, J. F. B. Mitchell, R. J. Stouffer, and K. E.  
250 Taylor (2007a), The WCRP CMIP3 multi-model dataset: a new era in climate change research,  
251 *Bull. Amer. Meteor. Soc.*, *88*, 1383-1394.

252 Meehl, G. A., and coauthors (2007b), Global climate projections, in *Climate Change 2007: The*  
253 *Physical Science Basis*, edited by S. Solomon et al., pp. 747-845, Cambridge University Press,  
254 Cambridge, UK.

255 Neelin, J. D., M. Munnich, H. Su, J. E. Meyerson, and C. E. Holloway (2006), Tropical drying trends  
256 in global warming models and observations, *Proc. Nat. Acad. Sci.*, *103*, 6110-6115.

257 Previdi, M., and B. G. Liepert, (2007), Annular modes and Hadley cell expansion under global

258 warming, *Geophys. Res. Lett.*, *34*, L22701, doi:10.1029/2007GL031243.

259 Scheff, J., and D. Frierson (2012), Twenty-first-century multimodel subtropical precipitation declines  
 260 are mostly midlatitude shifts, *J. Clim.*, in press, doi:10.1175/JCLI-D-11-00393.1.

261 Seager, R., and coauthors (2007), Model projections of an imminent transition to a more arid climate in  
 262 southwestern North America, *Science*, *316*, 1181-1184.

263 Seager, R., N. Naik, and G. A. Vecchi (2010), Thermodynamic and dynamic mechanisms for large-  
 264 scale changes in the hydrological cycle in response to global warming, *J. Clim.*, *23*, 4651-4668.

265 Seth, A., S. Rauscher, M. Rojas, S. Camargo, and A. Giannini (2011), Enhanced spring convective  
 266 barrier for monsoons in a warmer world?, *Clim. Change Lett.*, *104*, 403-414.

267 Seth, A., S. Rauscher, A. Giannini, S. Camargo, M. Biasutti, and M. Rojas (2012), Springtime drying in  
 268 monsoon regions in a warmer world: a CMIP5 analysis of ESMs and CMs, paper presented at  
 269 WCRP Workshop on CMIP5 Model Analysis, World Clim. Res. Prog., Honolulu, Hawaii.

270 Taylor, K. E., R. J. Stouffer, and G. A. Meehl (2012), An overview of CMIP5 and the experiment  
 271 design, *Bull. Amer. Meteor. Soc.*, *93*, 485-498.

272 Tyson, P. D., and R. H. Preston-Whyte (2000), *The Weather and Climate of Southern Africa*, Oxford  
 273 University Press, Cape Town.

274 Vecchi, G. A., and B. J. Soden (2007), Global warming and the weakening of the tropical circulation, *J.*  
 275 *Clim.*, *20*, 4316-4340.

276 Yin, J. (2005), A consistent poleward shift of the storm tracks in simulations of 21st century climate,  
 277 *Geophys. Res. Lett.*, *32*, L18701, doi:10.1029/2005GL023684.

278 **Table 1: List of CMIP5 models analyzed in this study**

279

Model name	Modeling group
ACCESS1.0	Commonwealth Scientific and Industrial Research Organization (CSIRO) and Bureau of Meteorology (BOM), Australia
BCC-CSM1.1	Beijing Climate Center, China Meteorological Administration
BNU-ESM	College of Global Change and Earth System Science, Beijing Normal

	University
CanESM2	Canadian Centre for Climate Modelling and Analysis
CCSM4	National Center for Atmospheric Research, USA
CESM1(BGC), CESM1(CAM5), CESM1(WACCM) <sup>a</sup>	Community Earth System Model Contributors, USA
CMCC-CM	Centro Euro-Mediterraneo per i Cambiamenti Climatici, Italy
CNRM-CM5	Centre National de Recherches Météorologiques / Centre Européen de Recherche et Formation Avancées en Calcul Scientifique, France
CSIRO-Mk3.6.0	Commonwealth Scientific and Industrial Research Organization / Queensland Climate Change Centre of Excellence, Australia
FGOALS-g2	LASG, Institute of Atmospheric Physics, Chinese Academy of Sciences and CESS, Tsinghua University
FGOALS-s2	LASG, Institute of Atmospheric Physics, Chinese Academy of Sciences
FIO-ESM	The First Institute of Oceanography, SOA, China
GFDL-CM3, GFDL-ESM2G, GFDL-ESM2M	NOAA Geophysical Fluid Dynamics Laboratory, USA
GISS-E2-R	NASA Goddard Institute for Space Studies, USA
HadGEM2-AO	National Institute of Meteorological Research/Korea Meteorological Administration
HadGEM2-CC, HadGEM2-ES	Met Office Hadley Centre, United Kingdom
INM-CM4	Institute for Numerical Mathematics, Russia
IPSL-CM5A-LR, IPSL-CM5A-MR, IPSL-CM5B-LR	Institut Pierre-Simon Laplace, France
MIROC-ESM, MIROC-ESM-CHEM, MIROC5	Japan Agency for Marine-Earth Science and Technology, Atmosphere and Ocean Research Institute (The University of Tokyo), and National Institute for Environmental Studies
MPI-ESM-LR, MPI-ESM-MR	Max Planck Institute for Meteorology, Germany
MRI-CGCM3	Meteorological Research Institute, Japan
NorESM1-M	Norwegian Climate Centre

280 <sup>a</sup>Run 1 (as specified in SF12) was not fully available for CESM1-WACCM at the time of submission,  
281 so run 2 was used instead.

282

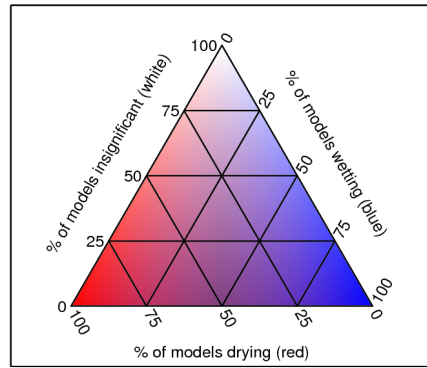
283 **Figure Captions**

284 **Figure 1.** In each season, black contours are the 1980-1999 CMIP5 multimodel climatological P (1,2,5  
285 mm/day lightest to boldest.) At each point, the colored shading shows the proportion of CMIP5 models  
286 for which the rcp8.5 1980-2099 seasonal P trend in the native model gridbox containing that point is  
287 negative and significant (red), positive and significant (blue), or insignificant (white), according to the  
288 legend.

289 **Figure 2.** For each season, 10°-wide longitude band, and meridional “location” relative to the  
290 individual models’ 1980-1999 climatological P features, the colored shading gives the CMIP5  
291 multimodel average frequencies of negative-and-significant (red), positive-and-significant (blue), and  
292 insignificant (white) rcp8.5 1980-2099 P trends in the individual model latitudes corresponding to that  
293 “location”. The color values are exactly as in figure 1. Longitude bands for which fewer than half of  
294 the models possess these climatological P features, and thus fewer than half of the models contribute to  
295 the plotted values, are struck through in cyan as a warning. For more detailed information, see the  
296 appendix, and see *Scheff and Frierson* [2012].

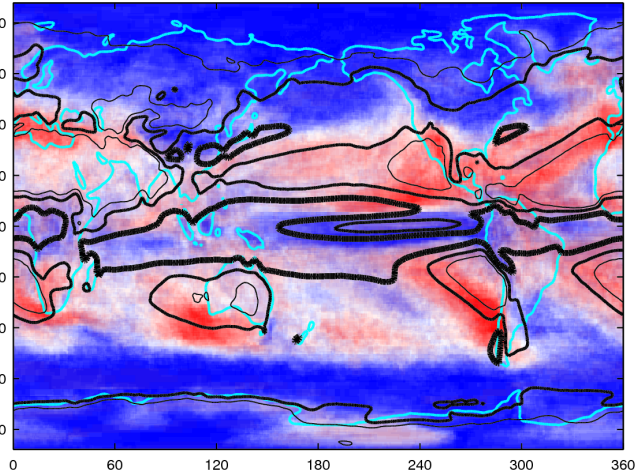
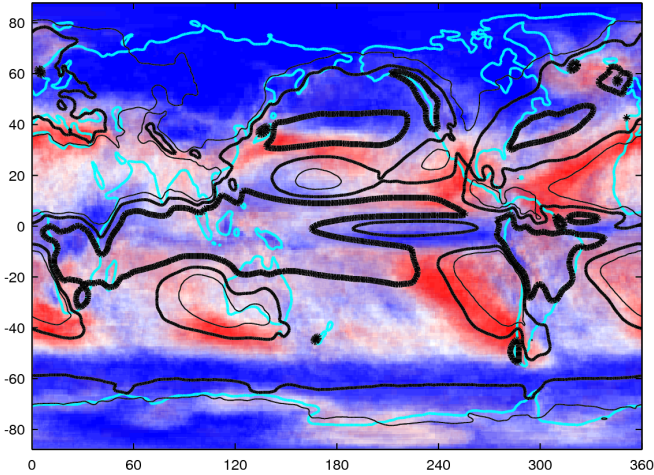
297

298  
299  
300  
301  
302  
303  
304  
305  
306  
307



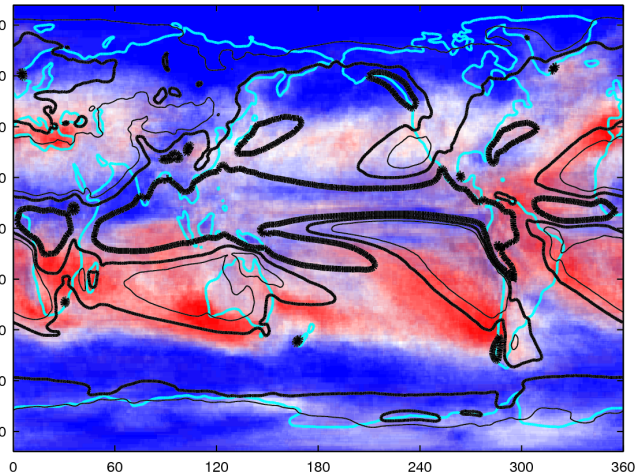
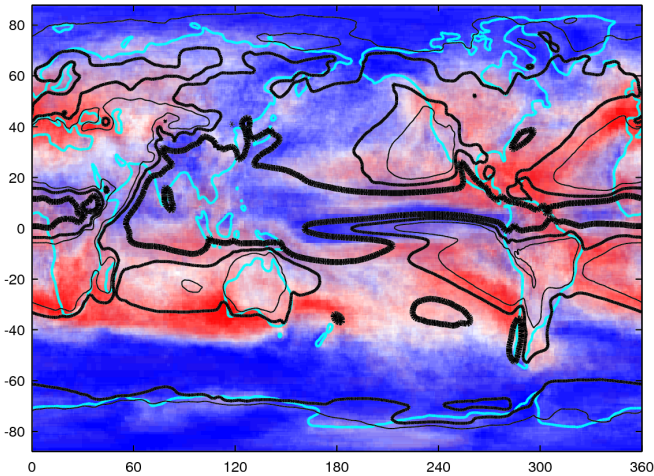
a) December-February

b) March-May

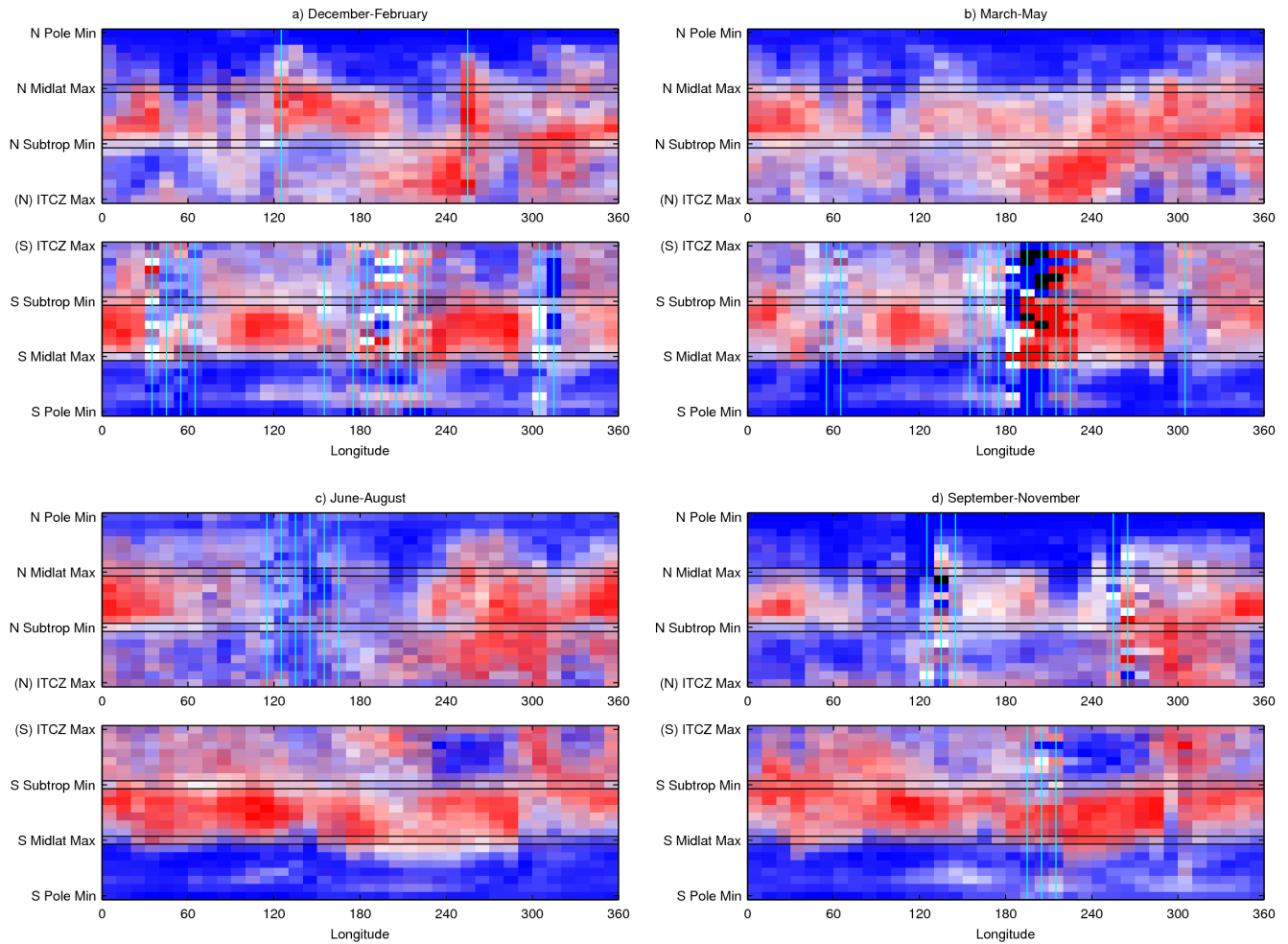


c) June-August

d) September-November



309 **Figure 1.** In each season, black contours are the 1980-1999 CMIP5 multimodel climatological P (1,2,5  
310 mm/day lightest to boldest.) At each point, the colored shading shows the proportion of CMIP5 models  
311 for which the rcp8.5 1980-2099 seasonal P trend in the native model gridbox containing that point is  
312 negative and significant (red), positive and significant (blue), or insignificant (white), according to the  
313 legend.  
314



316 **Figure 2.** For each season, 10°-wide longitude band, and meridional “location” relative to the  
 317 individual models’ 1980-1999 climatological P features, the colored shading gives the CMIP5  
 318 multimodel average frequencies of negative-and-significant (red), positive-and-significant (blue), and  
 319 insignificant (white) rcp8.5 1980-2099 P trends in the individual model latitudes corresponding to that  
 320 “location”. The color values are exactly as in figure 1. Longitude bands for which fewer than half of  
 321 the models possess these climatological P features, and thus fewer than half of the models contribute to  
 322 the plotted values, are struck through in cyan as a warning. For more detailed information, see the  
 323 appendix, and see *Scheff and Frierson* [2012].